

Synergistic Pd/Cu-catalyzed enantioselective Csp²-F bond alkylation of fluoro-1,3-dienes with aldimine esters

Huimin Yu¹, Qinglong Zhang¹ & Weiwei Zi^{1,2}  

Due to high bond dissociation energies of Csp²-F bonds, using fluorinated compounds in Csp²-Csp³ cross-coupling is difficult. Here the authors report a protocol for enantioselective Csp²-Csp³ coupling of dienyl fluorides with aldimine esters, enabled by synergistic copper and palladium catalysis. This reaction represents the first example of asymmetric Csp²-Csp³ cross-coupling involving an inert Csp²-F bond and provides expeditious access to chiral α -alkenyl α -amino acids with high enantioselectivity. Control experiments suggest that the Csp²-F bond activation occurs through a pathway involving PdH migratory insertion and subsequent allylic defluorination, rather than by direct oxidative addition of the Csp²-F bond to Pd(O). The detailed mechanism is further investigated by DFT calculation and the enantioselectivity is rationalized.

¹State Key Laboratory and Institute of Elemento-Organic Chemistry, College of Chemistry, Nankai University, Tianjin 300071, China. ²Haihe Laboratory of Sustainable Chemical Transformations, Tianjin 300071, China. ✉email: zi@nankai.edu.cn

Transition-metal-catalyzed enantioselective cross-coupling reactions between Csp^2-X compounds ($X = \text{halogen}$) and enolizable carbonyl compounds are commonly used transformations for asymmetric construction Csp^2-Csp^3 bonds^{1–7}. Many successful examples of this method have been reported, including pioneering work by the research groups of Ma¹, Hartwig², and Buchwald^{3,6}, who used chiral-ligand-bearing transition metals such as Cu and Pd to achieve enantiocontrol (Fig. 1a). These reactions initiated with oxidative addition of Csp^2-X bond to the Pd(0) or Cu(I), followed by ligand exchange and reductive elimination to form the Csp^2-Csp^3 bond. Halogenated compounds with Csp^2-I , Csp^2-Br , and even Csp^2-Cl bonds are suitable reaction substrates. However, because Csp^2-F bonds have high energies (120–129 kcal/mol for olefinic C–F bonds), fluorinated compounds have rarely been used as coupling partners^{8–15}.

Recently, C–F activation has been an important research topic in synthetic organic chemistry^{16–20}. One of the most successful strategies in this area is using transition-metal-mediated or -catalyzed metal–Nu insertion/ β -F elimination process²¹. Trifluoro-, difluoroalkenes have been intensively investigated for this purpose during the past few years^{22–30}; however, monofluoroalkenes are rarely explored class of compounds for similar C–F activation reactions (Fig. 1b). Moreover, despite those achievements in defluorinative carbon–carbon and carbon–heteroatom bond formation, enantioselective variants have seldom been realized. We envisioned that if an ingenious insertion/ β -F elimination mechanism was designed together with a suitable chiral induction strategy, the aforementioned challenged defluorinative Csp^2-Csp^3 coupling might be achieved.

In this work, we report a Cu/Pd cooperative system³¹ for enantioselective Csp^2-Csp^3 cross-coupling between dienyl fluorides and aldimine esters (Fig. 1c). Experimental and computational studies revealed that this reaction involved a unique Pd–H insertion/allylic defluorination process. This work not only represents the first example of enantioselective defluorinative Csp^2-Csp^3 coupling but also provides a highly efficient catalytic method to prepare chiral α -alkenyl α -amino acids (α -AAs), which

are important synthetic targets^{32–36} because of their potential biochemical and pharmacological activities³⁷.

Results and discussion

Reaction development. Our studies begin with investigating the reaction of dienyl fluoride *E*-**1a** with aldimine ester^{38–40} **2a** to generate α -alkenyl, α -methyl α -AA **3aa**. Using the stereocontrol exhibited by Cu-azomethine ylides in two-metal catalytic systems^{41–43}, we designed a synergistic Pd/Cu catalyst system^{44–55} for controlling the stereochemistry of the newly formed chiral center by means of an appropriate combination of ligands on the two metals during the coupling step (Table 1). First, we tested Phosferrox Cu complex L1–Cu with Pd catalysts bearing a bisphosphine ligand (dppe, dppp, Xantphos, or DPEphos);

Table 1 Optimization of catalyst system for the cross-coupling reaction.

Entry ^a	Pd catalyst	Cu catalyst	Yield [%] ^b	ee [%] ^c
1	L4-Pd	L1-Cu	<5	<i>n.d.</i>
2	L5-Pd	L1-Cu	<5	<i>n.d.</i>
3	L6-Pd	L1-Cu	<5	<i>n.d.</i>
4	L7-Pd	L1-Cu	<5	<i>n.d.</i>
5	L8-Pd	L1-Cu	53	96
6	L9-Pd	L1-Cu	50	98
7	L10-Pd	L1-Cu	73	99
8	L11-Pd	L1-Cu	87	96
9	L11-Pd	L2-Cu	75	98
10	L11-Pd	L3-Cu	86	99
11	<i>ent</i> - L11-Pd	L3-Cu	82	93
12	L11-Pd	—	<i>n.r.</i>	<i>n.d.</i>
13	—	L3-Cu	<i>n.r.</i>	<i>n.d.</i>

n.d. not determined, *n.r.* no reaction.

^aReaction conditions: (i) **1a** (0.2 mmol), **2a** (0.1 mmol), Pd catalyst (4 mol%), Cu catalyst (5 mol%), Et₃N (200 mol%), THF (0.5 mL), 30 °C, 24 h; (ii) citric acid (10 wt%, 4 mL).

^bIsolated yields are provided.

^cThe ee values were determined by HPLC using a column with a chiral stationary phase.

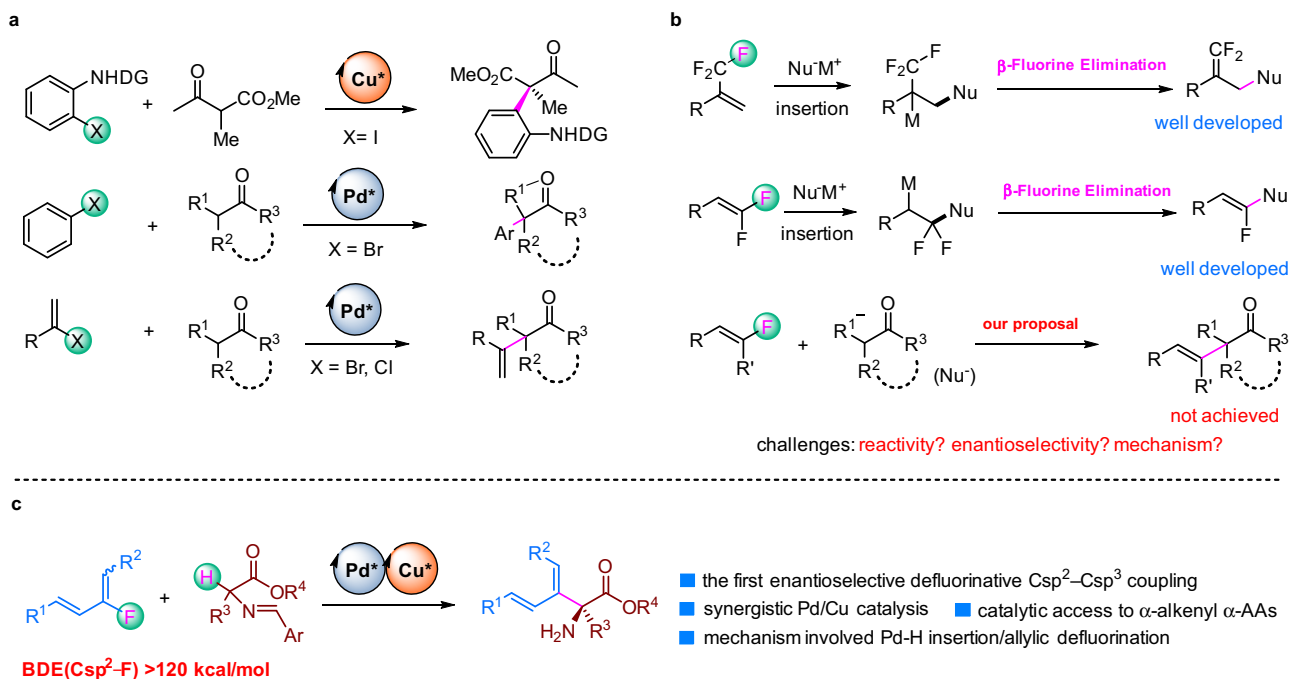


Fig. 1 Transition-metal-catalyzed asymmetric Csp^2-Csp^3 cross-coupling reactions. **a** Enantioselective Csp^2-Csp^3 cross-coupling of Csp^2-I (Br, Cl) Bonds. **b** C–F bond Activation by Nu–M Insertion/ β -fluorine elimination. **c** This work: C–F bond activation by Pd–H insertion/allylic defluorination for Csp^2-Csp^3 cross-coupling.

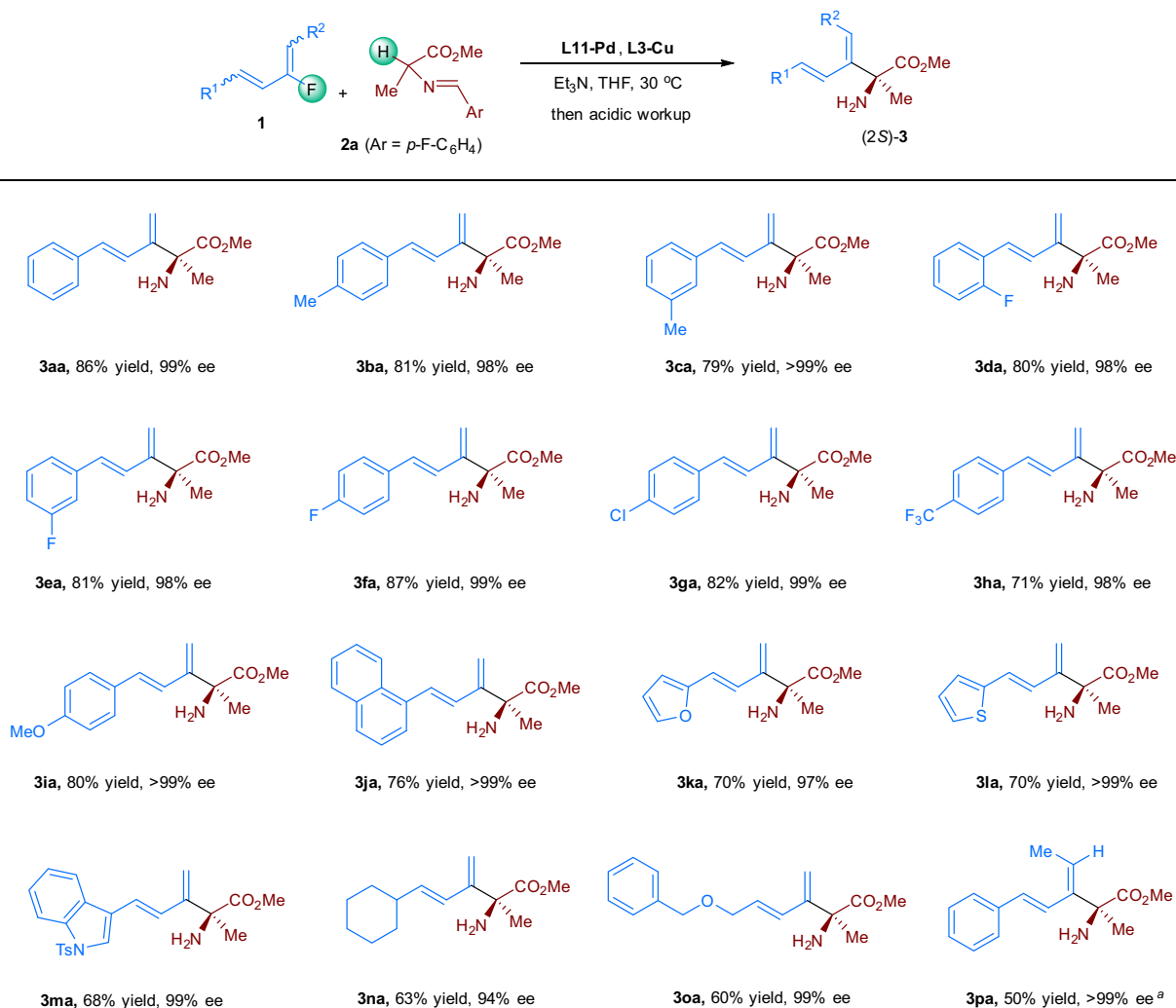


Fig. 2 Substrate scope with respect to the dienyl fluorides. Reaction conditions: (i) **1a** (0.4 mmol), **2a** (0.2 mmol), **L11-Pd** (4 mol%), **L3-Cu** (5 mol%), Et₃N (200 mol%), THF (0.5 mL), 30 °C, 24 h; (ii) citric acid (10 wt%, 4 mL). Isolated yields are provided. The ee values were determined by HPLC on a column with a chiral stationary phase. ^a**L11-Pd** (8 mol%), **L3-Cu** (10 mol%), THF (0.2 mL), 40 °C, 120 h.

L4-Pd–L7-Pd, respectively) and found that none of these combinations catalyzed the desired reaction (entries 1–4). In contrast, BINAP-ligated catalyst **L8-Pd** afforded **3aa** in 53% yield with 96% ee (entry 5). SEGPHOS- and Biphep-derived catalysts (**L9-Pd–L11-Pd**, entries 6–8) were also examined, and **L11-Pd** gave the best yield of the product. Subsequent tests of **L11-Pd** in combination with other Cu catalysts (**L2-Cu** and **L3-Cu**, entries 9 and 10) revealed that **L11-Pd/L3-Cu** gave the best results (86% yield, 99% ee). A slight decrease in enantioselectivity was observed when the opposite enantiomer of the Pd catalyst (*ent*-**L11-Pd**) was used together with **L3-Cu** (entry 11). This result implies the enantioselectivity was mainly controlled by the chiral Cu catalyst but the mismatched chirality between the two catalysts was slightly deleterious to the enantiocontrol.

Substrate scope. Having developed an effective dual-metal catalyst system, we investigated the substrate scope of the reaction, starting with dienyl fluorides **1** bearing various R¹ and R² substituents (Fig. 2). Phenyl rings with a methyl group (**3ba**, **3ca**), a fluorine atom (**3da–3fa**), a chlorine atom (**3ga**), a trifluoromethyl group (**3ha**), or a methoxy group (**3ia**) were well tolerated, regardless of the location of the substituent, affording the corresponding coupling products in 71–87% yields with

enantioselectivities exceeding 98% ee. Replacing the phenyl ring with a different aromatic ring—naphthyl (**3ja**), furyl (**3ka**), thiophenyl (**3la**), or indolyl (**3ma**)—had little influence on the reaction outcome, the corresponding α -alkenyl, α -alkyl α -AAs were obtained with excellent enantioselectivities. An alkyl-substituted substrate (R¹ = cyclohexyl) furnished **3na** in 63% yield, albeit with a reduced ee (94%). Even though allylic ethers are commonly sensitive to Pd owing to the possibility of C–O bond cleavage, a substrate with an allylic BnO ether moiety was well tolerated in this reaction system, giving **3oa** in 60% yield with 99% ee. A 1,4-disubstituted dienyl fluoride (R¹ = Ph, R² = Me) was also investigated, which afforded the desired product **3pa** in 50% yield with >99% ee. To determine the stereochemistry of the product, we converted **3aa** to its *p*-toluenesulfonamide derivative and confirmed its structure by means of X-ray crystallographic analysis, which allowed us to assign the absolute configuration as 2*S*.

Next, we probed the scope of aldimine ester substrate (Fig. 3). When R⁴ was methyl, R³ could be Et (**3ab**), ^{*n*}Bu (**3ac**), or phenylethyl (**3ad**). Heteroatom-tethered alkyl chains were also well-tolerated, as indicated by the formation of coupling products **3ae–3ag** in moderate to good yields with good enantioselectivities. In addition, we investigated compounds with various alkyl R⁴

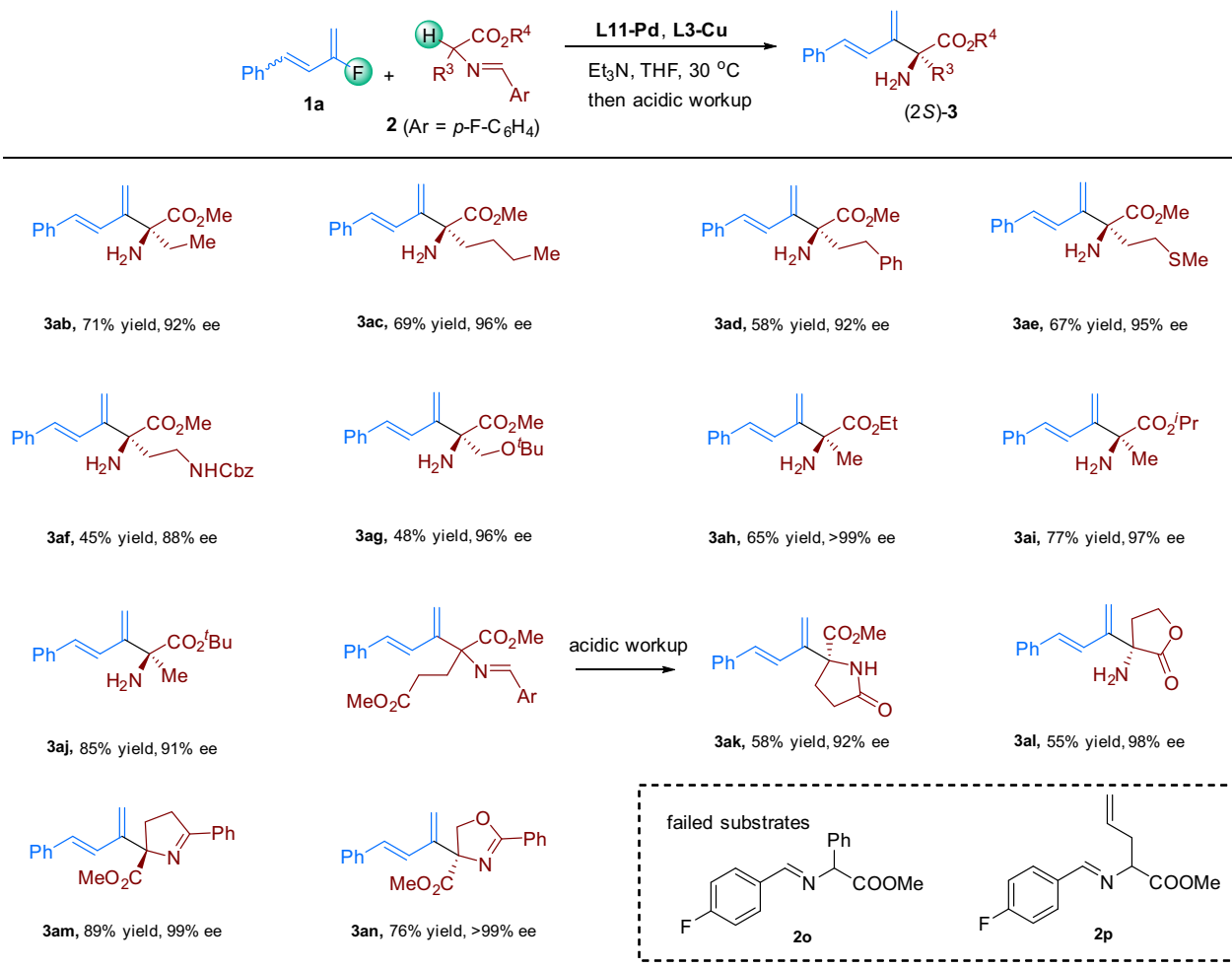


Fig. 3 Substrate scope with respect to the aldimine esters. Reaction conditions: (i) **1a** (0.4 mmol), **2a** (0.2 mmol), **L11-Pd** (4 mol%), **L3-Cu** (5 mol%), Et₃N (200 mol%), THF (0.5 mL), 30 °C, 48 h; (ii) citric acid (10 wt%, 4 mL). Isolated yields are provided. The ee values were determined by HPLC on a column with a chiral stationary phase.

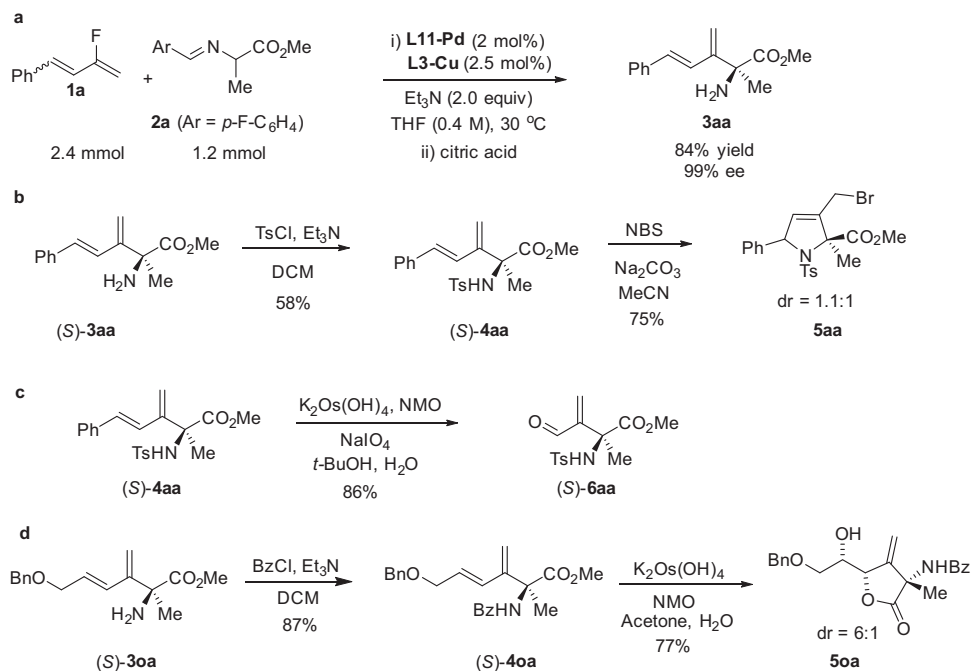


Fig. 4 Synthetic application. **a** Scale-up reaction at lower catalyst loading. **b** Intramolecular bromoamination reaction. **c** Selective cleavage of the internal alkene. **d** Dihydroxylation/lactonization reaction.

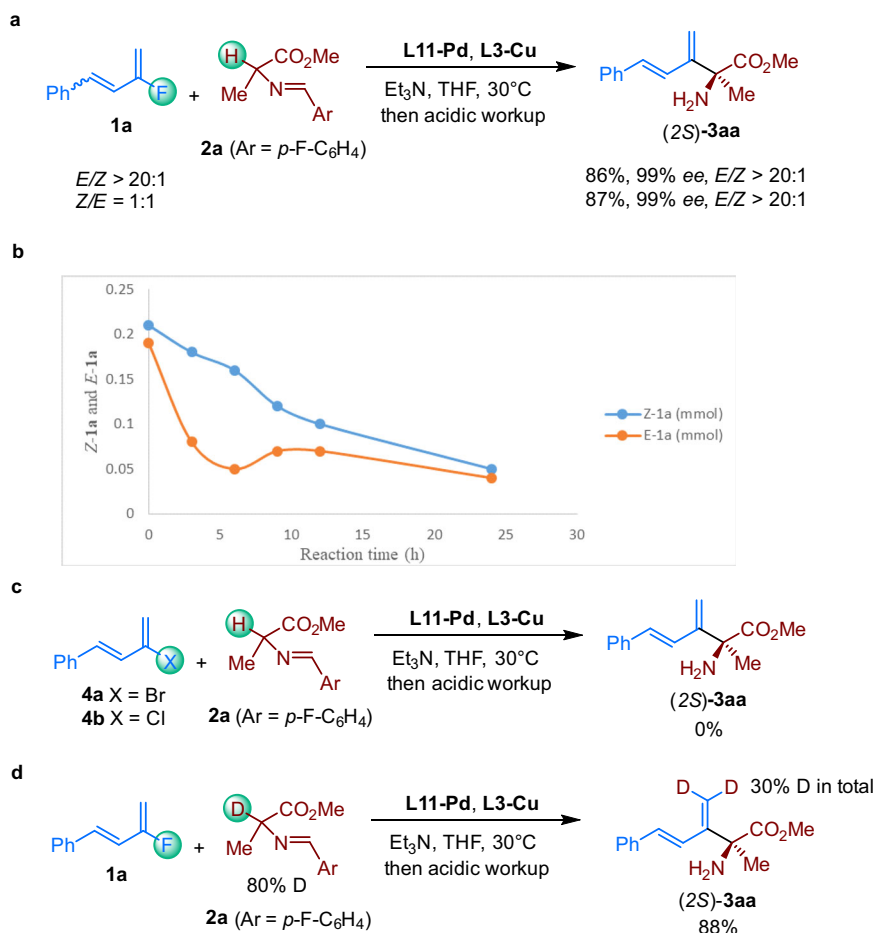


Fig. 5 Control experiments. **a** Relationship between the ratio of *Z/E*-**1a** and ratio of *Z/E*-**3aa**. **b** The absolute amount the *Z*-**1a** and *E*-**1a** during the reaction. **c** Reaction of diene bromide **4a** or diene chloride **4b** under the standard conditions. **d** Deuterium atom scramble experiment.

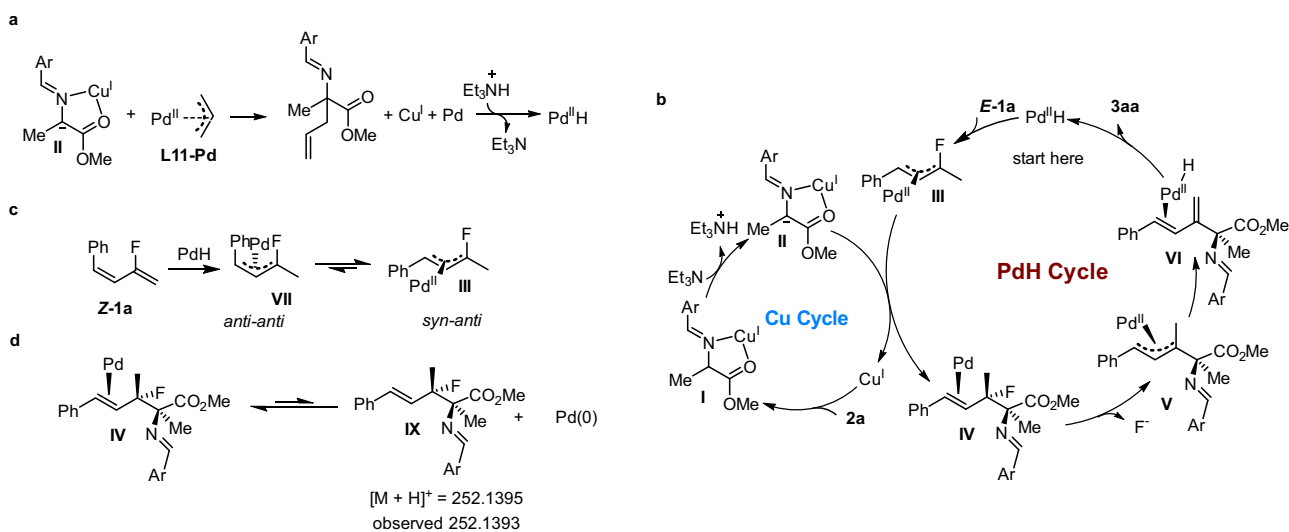


Fig. 6 Proposed mechanism. **a** Initial generation of PdH catalyst from the precatalyst **L11-Pd**. **b** Proposed catalytic cycle. **c** Isomerization of *anti-anti* π -allyl-Pd to *syn-anti* π -allyl-Pd. **d** HRMS detection of $[M + H]^+$ for Intermediate IX. The ligands were omitted for clarity.

groups (**3ah–3aj**), revealing that the reaction was not sensitive to the steric bulk of the ester. An aldimine ester derived from glutamic acid also reacted smoothly but gave lactam **3ak** in 58% yield with 92% ee, as a result of cyclization during the acidic workup. α -Amino- γ -butyrolactone derived imine underwent reaction with

1a to give **3al** in moderate yield. In addition to aldimine ester, cyclic ketimine ester and oxazoline ester were also compatible reaction partners. As shown in the formation of **3am** and **3an**, both the yields and enantioselectivities were well maintained for these types of nucleophiles. Phenylalanine derived aldimine ester **2o** failed to

undergo this transformation due to the steric bulk, and substrate **2p** bearing allyl group only gave complexed products, probably because the isomerization of the terminal olefin moiety.

Synthetic application. The reaction was scaled up to more than one mmol scale with a reduced catalyst loading [**L11-Pd** (2 mol%) and **L3-Cu** (2.5 mol%)] and the yield and enantioselectivity were well maintained (Fig. 4a). To demonstrate the utility of the reaction, the coupling products were transformed to other chiral scaffolds. Protection (*S*)-**3aa** with *p*-tolylsulfonyl group gave (*S*)-**4aa**, and the latter was treatment with NBS/Na₂CO₃ in acetonitrile to elaborate the bromoamination product **5aa** in 75% yield (Fig. 4b). The internal alkene moiety of (*S*)-**4aa** could be selectively cleaved with K₂Os(OH)₄/NMO, followed by NaIO₄, affording aldehyde (*S*)-**6aa** in 86% yield (Fig. 4c). Moreover,

protection the amine of (*S*)-**3oa** with benzoyl group gave (*S*)-**4oa**, which was further subjected to sequential dihydroxylation/lactonization conditions to furnish densely functionalized lactone **5oa** with good diastereoselectivity (Fig. 4d).

Mechanistic studies. To gain insight into the mechanism, we carried out some control experiments. We found that reactions of both >20:1 and 1:1 *E/Z*-**1a** gave >20:1 *E/Z*-**3aa** with essentially identical yields and ee values (Fig. 5a). On the other hand, when **1a** with the *E/Z* ratio of 1:1.1 was subjected to the reaction, the absolute amount of the *Z*-**1a** and *E*-**1a** was monitored (Fig. 5b). Interestingly, the concentration of *Z*-**1a** and *E*-**1a** are both decreased during the reaction; however, the *E*-**1a** has a faster consumption rate than *Z*-**1a** did. Most importantly, an inflection point appeared around 5 h in the *E*-**1a** consumption curve. These results indicate a possibility that *E*-**1a** preferentially reacted under the optimized conditions at the early stage, and *Z*-**1a** gradually isomerized to *E*-**1a**. In addition, when diene bromide **4a** or diene chloride **4b** was subjected to the reaction conditions, almost none of the coupling product (**3aa**) was observed (Fig. 5c). Consequently, we reasoned that direct oxidative addition of the Csp²-F bond to Pd(0) was probably not involved in the reaction pathway^{56,57}. Finally, the reaction between **1a** and deuterium-labeled **2a** resulted in the incorporation of a total 30% of the deuterium at the terminal carbon of the double bond in the coupling product (Fig. 5d). As a result, we speculated that a Pd-D insertion process might be involved in the reaction, which would lead to deuterium enriching at the terminus of the alkenes⁵⁸.

Based on the above-described results, as well as our previous studies^{59,60} on synergistic Pd/Cu-catalyzed coupling reactions of aldimine esters with unsaturated compounds, we proposed that this coupling reaction proceeds based on a mechanism involving the Cu and PdH cycles shown in Fig. 6. In the Cu catalytic cycle, Cu acts as a Lewis acid to activate aldimine ester **2a** to form metallated azomethine ylide **II**, which serves as a nucleophile in the coupling reaction. Alkylation of **II** with pre-palladium catalyst **L11-Pd** forms the **L11-Pd(0)**, which then undergoes oxidative addition with

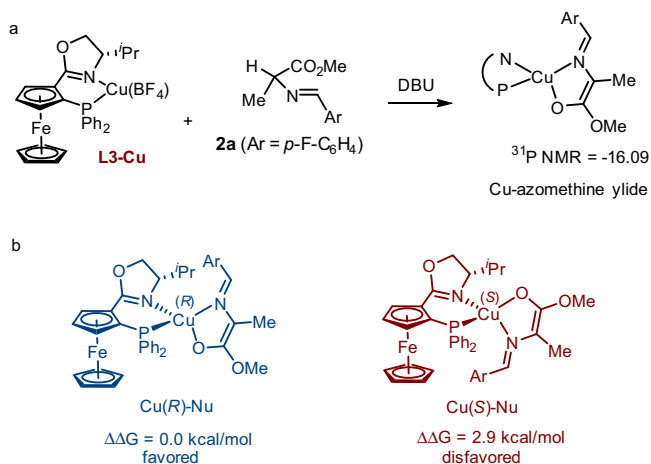


Fig. 7 Determination of the structure for the Cu-azomethine ylide.

a Observation of the Cu-azomethine ylide by ³¹P NMR. **b** Energy comparison of Cu(R)-Nu and Cu(S)-Nu.

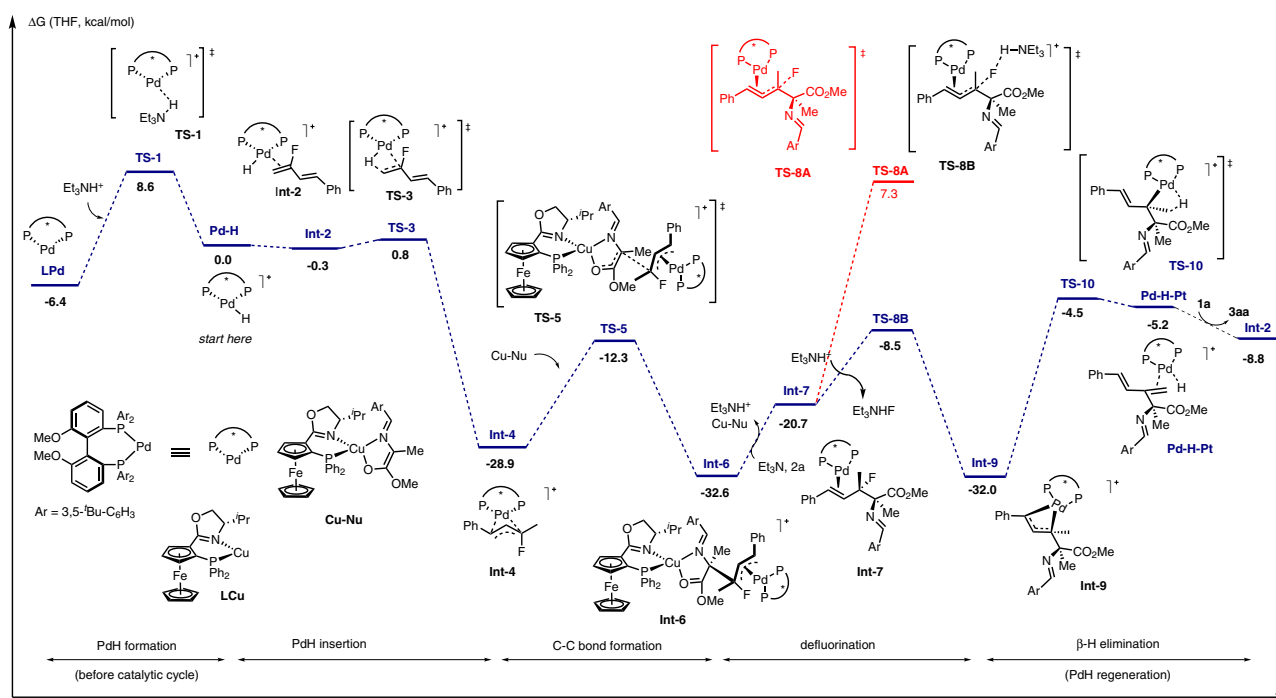


Fig. 8 Energy profile for the proposed mechanism. Calculations were carried out at the M06-2x(SMD)/def2-TZVP//B3LYP-D3BJ/6-31 g(d)/LanL2dz level of theory.

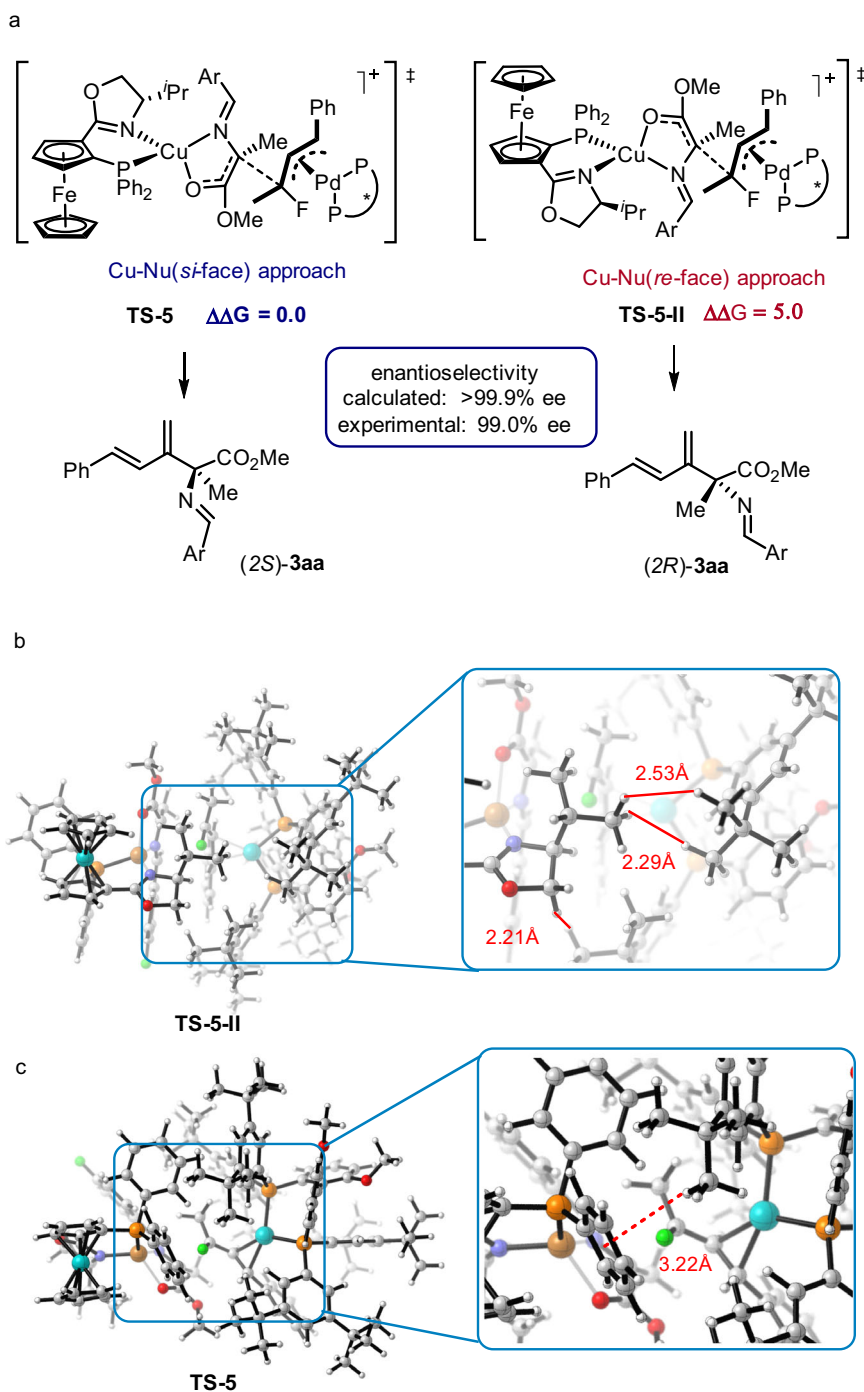


Fig. 9 Rationalization of the enantioselectivity. **a** Comparison of Transition states **TS-5** and **TS-5-II**. **b** Steric interaction between the oxazoline ring and *t*-Bu group in **TS-5-II**. **c** Attractive C-H...Ar interaction in **TS-5**.

Et_3NH^+ to generate the PdH catalyst (Fig. 6a). In the PdH catalytic cycle (Fig. 6b), PdH migratory insertion into the C=C bond of the vinyl fluoride moiety of *E*-**1a** generates fluorinated Pd-allyl **III**^{61–64}. An allylic substitution reaction between **III** and metallated azomethine ylide **II** affords Pd intermediate **IV** and regenerates the Cu catalyst. Intermediate **IV** undergoes rapid allylic defluorination, giving allyl-Pd **V**, which is converted to **VI** via β -H elimination. Product **3aa** dissociates from **VI**, and the PdH regenerated^{65–67}. For *Z*-**1a**, the *anti-anti* η^3 -Pd-allyl **VII** is generated after PdH migratory insertion, which equilibrates to thermodynamically more stable *syn-anti* η^3 -Pd-allyl **III** through η^3 - η^1 - η^3

isomerization (Fig. 6c). Therefore *Z*-**1a** would then undertake the same catalytic cycle to form the same *E*-type product **3aa**. This proposed mechanism was highly consistent with the controlled experiments in Fig. 3. Moreover, we observed a $[\text{M} + \text{H}]^+$ signal at 252.1393 in the HRMS spectrum of the reaction mixtures. This result indicates the formation of **IX**, which comes from the dissociation of Pd(0) from intermediate **IV** (Fig. 6d).

Computational studies. To further understand the mechanism, we performed DFT calculation to investigate the energy profile of

this reaction. Stoichiometric reaction of **L3-Cu** and substrate **2a** with DBU, only one isomeric Cu-azomethine ylide was formed, as indicated by a single ^{31}P NMR signal at -16.09 (Fig. 7). The structures of Cu-azomethine ylide featuring a (R)- or (S)- metal chirality were calculated and we found the former is 2.9 kcal/mol stable than the latter. Therefore, we rationalized that Cu(R)-Nu rather than Cu(S)-Nu was the form for nucleophile and therefore its structure was adopted for the remaining DFT calculation (Fig. 8).

As proposed in Fig. 8, the PdH was initially formed via oxidative protonation of Pd(0) with Et_3NH^+ . The transition state for this step was located as **TS-1**, which has an energy barrier of 15.0 kcal/mol. After being coordinated by substrate **2a**, the resulting intermediate **Int-2** occurs migratory insertion of the Pd-H bond into the terminal olefin moiety to afford π -allyl-Pd species **Int-4**. The energy barrier for this step is only 1.1 kcal/mol; however, the reserved β -H elimination step requires activation energy of 29.7 kcal/mol (**Int-4** \rightarrow **TS-3** \rightarrow **Int-2**). Therefore, the Pd-H migratory insertion is not a reversible process. The resulting **Int-4** accepts nucleophilic attack from the *si*-face of the metallated azomethine ylide Cu-Nu, to give C-C bond formation intermediate **Int-6**. Dissociation of LCu from **Int-6** affords species **Int-7**, which then undergoes allylic defluorination. The direct nucleophilic displacement/ionization mechanism for the defluorination transition state (**TS-8A**) has a high energy barrier of 28.0 kcal/mol. But a Et_3NH^+ mediated process, of which the transition state was located as **TS-8B**, only requires an activation barrier of 12.2 kcal/mol. The resulting **Int-9** then occurs β -H elimination step via **TS-10** with an energy barrier of 27.5 kcal/mol to elaborate product (2*S*)-**3aa** and regenerates the PdH catalyst.

To elucidate the enantioselectivity, the approach from the *re*-face of Cu-Nu during the C-C bond formation was also calculated and the transition state is identified as **TS-5-II** (Fig. 9a). Comparing the energies of **TS-5** and **TS-5-II**, the latter is disfavored over the former by 5.0 kcal/mol, which is in agreement with the experimental result that (2*S*)-**3aa** is formed with 99% ee. In the transition state structure **TS-5-II**, the oxazoline ring group on the phosphorox ligand has a very short distance away from *t*-Bu groups of DTB-Biphep and which leads to significant steric interaction between the two ligands (Fig. 9b). This repulsive interaction likely contributes to the higher energy observed for this competing transition state. In contrast, in the transition state structure **TS-5**, the electrophile approaches from the *si*-face of Cu-Nu which avoids the steric repulsion between the oxazoline ring and *t*-Bu groups. Moreover, an attractive C-H \cdots Ar interaction is observed in **TS-5**, which also contributes to a lower energy (Fig. 9c).

In summary, the first enantioselective defluorinative Csp^2 - Csp^3 cross-coupling was achieved by means of synergistic Cu/Pd-catalyzed asymmetric coupling between aldimine esters and dienyl fluorides. This reaction has a wide substrate scope and shows good to excellent enantioselectivities and it provides an efficient catalytic method for preparing chiral α -vinyl, α -alkyl α -amino acid derivatives. Both experimental and computational studies revealed that the reaction is initiated by a PdH migratory insertion, which is followed by nucleophilic allylic substitution by a Cu-azomethine ylide to form the C-C bond. Then a Pd/ Et_3NH^+ -mediated allylic defluorination undergoes, subsequently followed by a β -H elimination to elaborate the coupling product and regenerate the PdH catalyst.

Methods

General procedure for coupling of dienyl fluorides and aldimine esters. In glove box, Cu(MeCN) $_2$ PF $_6$ (3.7 mg, 0.01 mmol, 5 mol%) and chiral ligand (S_2S_2)-**L3** (5.3 mg, 0.011 mmol, 5.5 mol%) were dissolved in dry THF (0.4 M, 0.5 mL) and

stirred at room temperature for 0.5 h. To the solution, substrate aldimine esters **2** (0.2 mmol), Et_3N (0.4 mmol), dienes **1** (0.4 mmol) and palladium catalyst L11-Pd (10.1 mg, 0.008 mmol, 4 mol%) were added sequentially. The reaction mixture was stirred at 30 °C for 24 h. To the reaction mixture was added citric acid solution (4 mL, 10 wt%) and the mixture was stirred for 2 h. The mixture was neutralized with solid K_2CO_3 and extracted with EtOAc (10 mL \times 3). The combined extracts were dried over MgSO_4 and concentrated in vacuo to afford a residue. The residue was then purified by SiO_2 column chromatography to give the desired product.

Data availability

The authors declare that the data supporting the findings of this study are available within the article and its Supplementary Information Files as well as from the corresponding author on request. The Cartesian coordinates for the calculated structures are available within the Supplementary Data 1. The X-ray crystallographic coordinates for structure reported in this study have been deposited at the Cambridge Crystallographic Data Centre (CCDC), under deposition numbers CCDC 2036502 (*p*-toluenesulfonamide derivative of **3aa**). These data can be obtained free of charge from The Cambridge Crystallographic Data Centre via www.ccdc.cam.ac.uk/data_request/cif.

Received: 18 May 2021; Accepted: 12 April 2022;

Published online: 05 May 2022

References

- Xie, X., Chen, Y. & Ma, D. Enantioselective arylation of 2-methylacetoacetates catalyzed by CuI/*trans*-4-Hydroxy-L-proline at low reaction temperatures. *J. Am. Chem. Soc.* **128**, 16050–16051 (2006).
- Ge, S. & Hartwig, J. F. Nickel-catalyzed asymmetric α -arylation and heteroarylation of ketones with chloroarenes: effect of halide on selectivity, oxidation state, and room-temperature reactions. *J. Am. Chem. Soc.* **133**, 16330–16333 (2011).
- Zhu, Y. & Buchwald, S. L. Ligand-controlled asymmetric arylation of aliphatic α -amino anion equivalents. *J. Am. Chem. Soc.* **136**, 4500–4503 (2014).
- Jiao, Z., Chee, K. W. & Zhou, J. S. Palladium-catalyzed asymmetric α -arylation of alkylnitriles. *J. Am. Chem. Soc.* **138**, 16240–16243 (2016).
- Zhu, C., Wang, D., Zhao, Y., Sun, W.-Y. & Shi, Z. Enantioselective palladium-catalyzed intramolecular α -arylation desymmetrization of 1, 3-diketones. *J. Am. Chem. Soc.* **139**, 16486–16489 (2017).
- Taylor, A. M., Altman, R. A. & Buchwald, S. L. Palladium-catalyzed enantioselective α -arylation and α -vinylation of oxindoles facilitated by an axially chiral P-stereogenic ligand. *J. Am. Chem. Soc.* **131**, 9900–9901 (2009).
- Chieffi, A., Kamikawa, K., Åhman, J., Fox, J. M. & Buchwald, S. L. Catalytic asymmetric vinylation of ketone enolates. *Org. Lett.* **3**, 1897–1900 (2001).
- Ackermann, L., Born, R., Spatz, J. & Meyer, H. D. Efficient Aryl-(Hetero)Aryl coupling by activation of C-Cl and C-F Bonds Using Nickel Complexes of Air-Stable Phosphine Oxides. *Angew. Chem. Int. Ed.* **44**, 7216–7219 (2005).
- Yoshikai, N., Mashima, H. & Nakamura, E. Nickel-catalyzed cross-coupling reaction of aryl fluorides and chlorides with Grignard reagents under Nickel/Magnesium Bimetallic Cooperation. *J. Am. Chem. Soc.* **127**, 17978–17979 (2005).
- Yoshikai, N., Matsuda, H. & Nakamura, E. Hydroxyphosphine Ligand for Nickel-Catalyzed Cross-Coupling through Nickel/Magnesium Bimetallic Cooperation. *J. Am. Chem. Soc.* **131**, 9590–9599 (2009).
- Liu, X.-W., Echavarren, J., Zarate, C. & Martin, R. Ni-catalyzed borylation of aryl fluorides via C-F cleavage. *J. Am. Chem. Soc.* **137**, 12470–12473 (2015).
- Niwa, T., Ochiai, H., Watanabe, Y. & Hosoya, T. Ni/Cu-catalyzed defluoroborylation of fluoroarenes for diverse C-F bond functionalizations. *J. Am. Chem. Soc.* **137**, 14313–14318 (2015).
- Tobisu, M., Xu, T., Shimasaki, T. & Chatani, N. Nickel-catalyzed Suzuki-Miyaura reaction of aryl fluorides. *J. Am. Chem. Soc.* **133**, 19505–19511 (2011).
- Ho, Y. et al. Nickel-Catalyzed Csp^2 - Csp^3 bond formation via C-F bond activation. *Org. Lett.* **20**, 5644–5647 (2018).
- Butcher, T. W. et al. Desymmetrization of difluoromethylene groups by C-F bond activation. *Nature* **583**, 548–553 (2020).
- Amii, H. & Uneyama, K. C-F Bond Activation in Organic Synthesis. *Chem. Rev.* **109**, 2119–2183 (2009).
- Ahrens, T., Kohlmann, J., Ahrens, M. & Braun, T. Functionalization of fluorinated molecules by transition-metal-mediated C-F bond activation to access fluorinated building blocks. *Chem. Rev.* **115**, 931–972 (2015).
- Unzner, T. A. & Magauer, T. Carbon-fluorine bond activation for the synthesis of functionalized molecules. *Tetrahedron Lett.* **56**, 877–883 (2015).
- Shen, Q. et al. Review of recent advances in C-F bond activation of aliphatic fluorides. *J. Fluor. Chem.* **179**, 14–22 (2015).

20. Fu, L., Chen, Q. & Nishihara, Y. Recent advance in transition-metal-catalyzed C–C bond formation via C(sp²)-F bond cleavage. *Chem. Rec.* **21**, 1–18 (2021).
21. Fujita, T., Fuchibe, K. & Ichikawa, J. Transition-metal-mediated and -catalyzed C–F bond activation by fluorine elimination. *Angew. Chem. Int. Ed.* **58**, 390–402 (2019).
22. Ichitsuka, T., Fujita, T., Arita, T. & Ichikawa, J. Double C–F bond activation through β -fluorine elimination: Nickel-Mediated [3+2] cycloaddition of 2-Trifluoromethyl-1-alkenes with alkynes. *Angew. Chem. Int. Ed.* **53**, 7564–7568 (2014).
23. Thornbury, R. T. & Toste, F. D. Palladium-catalyzed defluorinative coupling of 1-Aryl-2,2-difluoroalkenes and boronic acids: stereoselective synthesis of monofluorostilbenes. *Angew. Chem. Int. Ed.* **55**, 11629–11632 (2016).
24. Tian, P., Feng, C. & Loh, T.-P. Rhodium-catalysed C(sp²)-C(sp²) bond formation via C–H/C–F activation. *Nat. Commun.* **6**, 7472 (2015).
25. Wu, J.-Q. et al. Experimental and theoretical studies on rhodium-catalyzed coupling of benzamides with 2,2-difluorovinyl tosylate: diverse synthesis of fluorinated heterocycles. *J. Am. Chem. Soc.* **139**, 3537–3545 (2017).
26. Lu, X. et al. Nickel-catalyzed defluorinative reductive cross-coupling of gem-difluoroalkenes with unactivated secondary and tertiary alkyl halides. *J. Am. Chem. Soc.* **139**, 12632–12637 (2017).
27. Sakaguchi, H. et al. Copper-catalyzed regioselective monodefluoroborylation of polyfluoroalkenes en route to diverse fluoroalkenes. *J. Am. Chem. Soc.* **139**, 12855–12862 (2017).
28. Zell, D. et al. Mild Cobalt(III)-Catalyzed Allylative C–F/C–H functionalizations at room temperature. *Chem. Eur. J.* **23**, 12145–12148 (2017).
29. Ma, Q., Wang, Y. & Tsui, G. C. Stereoselective palladium-catalyzed C–F bond alkylation of tetrasubstituted gem-difluoroalkenes. *Angew. Chem. Int. Ed.* **59**, 11293–11297 (2020).
30. Dai, W., Shi, H., Zhao, X. & Cao, S. Sterically controlled Cu-catalyzed or transition-metal-free cross-coupling of gem-Difluoroalkenes with tertiary, secondary, and primary alkyl grignard reagents. *Org. Lett.* **18**, 4284–4287 (2016).
31. Wu, Y., Huo, X. & Zhang, W. Synergistic Pd/Cu catalysis in organic synthesis. *Chem. Eur. J.* **26**, 4895–4916 (2020).
32. Armstrong, A. & Emmerson, D. P. G. Enantioselective synthesis of α -Alkyl, α -Vinyl Amino Acids via [2,3]-sigmatropic rearrangement of selenimides. *Org. Lett.* **13**, 1040–1043 (2011).
33. Berkowitz, D. B., Wu, B. & Li, H. A Formal [3,3]-sigmatropic rearrangement route to quaternary α -Vinyl Amino Acids: Use of Allylic N-PMP Trifluoroacetimidates. *Org. Lett.* **8**, 971–974 (2006).
34. Shea, R. G. et al. Allylic selenides in organic synthesis: new methods for the synthesis of allylic amines. *J. Org. Chem.* **51**, 5243–5252 (1986).
35. Genna, D. T., Hencken, C. P., Siegler, M. A. & Posner, G. H. α -Chloro- β , γ -ethylenic Esters: entiocontrolled synthesis and substitutions. *Org. Lett.* **12**, 4694–4697 (2010).
36. Panahi, F., Khosravi, H., Bauer, F. & Breit, B. Asymmetric hydroalkylation of alkynes and allenes with imidazolidinone derivatives: α -alkenylation of α -amino acids. *Chem. Sci.* **12**, 7388–7392 (2021).
37. Berkowitz, D. B., Charette, B. D., Karukurichi, K. R. & McFadden, J. M. α -Vinyl amino acids: occurrence, asymmetric synthesis, and biochemical mechanisms. *Tetrahedron: Asymmetry* **17**, 869–882 (2006).
38. Coldham, I. & Hufton, R. Intramolecular dipolar cycloaddition reactions of azomethine ylides. *Chem. Rev.* **105**, 2765–2810 (2005).
39. Narayan, R., Potowski, M., Jia, Z.-J., Antonchick, A. P. & Waldmann, H. Catalytic Enantioselective 1,3-Dipolar cycloadditions of azomethine ylides for biology-oriented synthesis. *Acc. Chem. Res.* **47**, 1296–1310 (2014).
40. Wei, L., Chang, X. & Wang, C.-J. Catalytic asymmetric reactions with N-metallated azomethine ylides. *Acc. Chem. Res.* **53**, 1084–1100 (2020).
41. Huo, X., Zhang, J., Fu, J. & Zhang, W. Ir/Cu dual catalysis: entio- and diastereodivergent access to α,α -disubstituted α -amino acids bearing vicinal stereocenters. *J. Am. Chem. Soc.* **140**, 2080–2084 (2018).
42. Wei, L., Zhu, Q., Xu, S.-M., Chang, X. & Wang, C.-J. Stereodivergent synthesis of α,α -disubstituted α -amino acids via synergistic Cu/Ir catalysis. *J. Am. Chem. Soc.* **140**, 1508–1513 (2018).
43. Peng, L., He, Z., Xu, X. & Guo, C. Cooperative Ni/Cu-catalyzed asymmetric propargylic alkylation of aldimine esters. *Angew. Chem. Int. Ed.* **59**, 14270–14274 (2020).
44. Nagra, F., Macé, Y., Lambin, D. & Riant, O. Copper/Palladium-Catalyzed 1,4 reduction and asymmetric allylic alkylation of α,β -unsaturated ketones: enantioselective dual catalysis. *Angew. Chem. Int. Ed.* **52**, 3208–3212 (2013).
45. Semba, K. & Nakao, Y. Arylboration of alkenes by cooperative palladium/copper catalysis. *J. Am. Chem. Soc.* **136**, 7567–7570 (2014).
46. Jia, T. et al. A Cu/Pd cooperative catalysis for enantioselective allylboration of alkenes. *J. Am. Chem. Soc.* **137**, 13760–13763 (2015).
47. Friis, S. D., Pirnot, M. T. & Buchwald, S. L. Asymmetric hydroarylation of vinylarenes using a synergistic combination of CuH and Pd catalysis. *J. Am. Chem. Soc.* **138**, 8372–8375 (2016).
48. Logan, K. M. & Brown, M. K. Catalytic enantioselective arylboration of alkenylarenes. *Angew. Chem. Int. Ed.* **56**, 851–855 (2017).
49. Saito, A., Kumagai, N. & Shibasaki, M. Cu/Pd synergistic dual catalysis: asymmetric α -allylation of an α -CF₃ amide. *Angew. Chem. Int. Ed.* **56**, 5551–5555 (2017).
50. Huo, X. et al. Stereoselective and site-specific allylic alkylation of amino acids and small peptides via a Pd/Cu dual catalysis. *J. Am. Chem. Soc.* **139**, 9819–9822 (2017).
51. Wei, L., Xu, S.-M., Zhu, Q., Che, C. & Wang, C.-J. Synergistic Cu/Pd catalysis for enantioselective allylic alkylation of aldimine esters: access to α,α -Disubstituted α -Amino Acids. *Angew. Chem. Int. Ed.* **56**, 12312–12316 (2017).
52. Yabushita, K., Yuasa, A., Nagao, K. & Ohmiya, H. Asymmetric catalysis using aromatic aldehydes as chiral α -alkoxyalkyl anions. *J. Am. Chem. Soc.* **141**, 113–117 (2019).
53. Liao, Y. et al. Enantioselective synthesis of multisubstituted allenes by cooperative Cu/Pd-Catalyzed 1,4-Arylboration of 1,3-Enynes. *Angew. Chem. Int. Ed.* **59**, 1176–1180 (2020).
54. Bai, X., Wu, C., Ge, S. & Lu, Y. Pd/Cu-catalyzed enantioselective sequential Heck/Sonogashira coupling: asymmetric synthesis of oxindoles containing Trifluoromethylated Quaternary Stereogenic Centers. *Angew. Chem. Int. Ed.* **59**, 2764–2768 (2020).
55. He, R. et al. Stereodivergent Pd/Cu catalysis for the dynamic kinetic asymmetric transformation of racemic unsymmetrical 1,3-disubstituted allyl acetates. *J. Am. Chem. Soc.* **142**, 8097–8103 (2020).
56. de Jong, G. T. & Bickelhaupt, F. M. Oxidative addition of the fluoromethane C–F Bond to Pd. An ab Initio Benchmark and DFT validation study. *J. Phys. Chem. A* **109**, 9685–9699 (2005).
57. Rekhroukh, F., Chen, W., Brown, R. K., White, A. J. P. & Crimmin, M. R. Palladium-catalysed C–F alumination of fluorobenzenes: mechanistic diversity and origin of selectivity. *Chem. Sci.* **11**, 7842–7849 (2020).
58. Wang, H., Zhang, R., Zhang, Q. & Zi, W. Synergistic Pd/Amine-catalyzed stereodivergent hydroalkylation of 1,3-dienes with aldehydes: reaction development, mechanism, and stereochemical origins. *J. Am. Chem. Soc.* **143**, 10948–10962 (2021).
59. Zhang, Q., Yu, H. & Zi, W. Stereodivergent coupling of 1,3-dienes with aldimine esters enabled by synergistic Pd and Cu catalysis. *J. Am. Chem. Soc.* **141**, 14554–14559 (2019).
60. Zhu, M., Zhang, Q. & Zi, W. Diastereodivergent synthesis of β -Amino alcohols by dual-metal-catalyzed coupling of alkoxyallenes with aldimine esters. *Angew. Chem. Int. Ed.* **60**, 6545–6552 (2021).
61. Liao, L. & Sigman, M. S. Palladium-catalyzed hydroarylation of 1,3-dienes with boronic esters via reductive formation of π -Allyl palladium intermediates under oxidative conditions. *J. Am. Chem. Soc.* **132**, 10209–10211 (2010).
62. Zhou, H., Wang, Y., Zhang, L., Cai, M. & Luo, S. Enantioselective terminal addition to allenes by dual chiral primary amine/palladium catalysis. *J. Am. Chem. Soc.* **139**, 3631–3634 (2017).
63. Adamson, N. J., Wilbur, K. C. E. & Malcolmson, S. J. Enantioselective intermolecular Pd-catalyzed hydroalkylation of acyclic 1,3-dienes with activated pronucleophiles. *J. Am. Chem. Soc.* **140**, 2761–2764 (2018).
64. Park, S., Adamson, N. J. & Malcolmson, S. J. Brønsted acid and Pd-PHOX dual-catalysed enantioselective addition of activated C-pronucleophiles to internal dienes. *Chem. Sci.* **10**, 5176–5182 (2019).
65. Adamson, N., Hull, E. & Malcolmson, S. J. Enantioselective intermolecular addition of aliphatic amines to acyclic dienes with a Pd-PHOX catalyst. *J. Am. Chem. Soc.* **139**, 7180–7183 (2017).
66. Nie, S.-Z., Davison, R. T. & Dong, V. M. Enantioselective coupling of dienes and phosphine oxides. *J. Am. Chem. Soc.* **140**, 16450–16454 (2018).
67. Zhang, Q., Dong, D. & Zi, W. Palladium-catalyzed regio- and enantioselective hydrosulfonylation of 1,3-dienes with sulfinic acids: scope, mechanism, and origin of selectivity. *J. Am. Chem. Soc.* **142**, 15860–15869 (2020).

Acknowledgements

This work was supported by the National Natural Science Foundation of China (nos. 21871150, 22071118, for W.Z. and 22001130 for Q.Z.) and the Fundamental Research Funds for Central University. H.Y. was supported by “Tianjin Research Innovation Project for Postgraduate Students” (no. 2019YJSB072). Q.Z. was supported by the China Postdoctoral Science Foundation (no. 2019M660973). We thank the Haihe Laboratory of Sustainable Chemical Transformations for financial support (no. ZYTS202101).

Author contributions

W.Z. conceived and tutored this work. Q.Z. conducted preliminary studies and co-tutored this work. H.Y. performed all the experiments and prepared the Supplementary Information. All the authors co-wrote this manuscript.

Competing interests

The authors declare no competing interests.

Additional information

Supplementary information The online version contains supplementary material available at <https://doi.org/10.1038/s41467-022-30152-7>.

Correspondence and requests for materials should be addressed to Weiwei Zi.

Peer review information *Nature Communications* thanks the anonymous reviewer(s) for their contribution to the peer review of this work.

Reprints and permission information is available at <http://www.nature.com/reprints>

Publisher's note Springer Nature remains neutral with regard to jurisdictional claims in published maps and institutional affiliations.



Open Access This article is licensed under a Creative Commons Attribution 4.0 International License, which permits use, sharing, adaptation, distribution and reproduction in any medium or format, as long as you give appropriate credit to the original author(s) and the source, provide a link to the Creative Commons license, and indicate if changes were made. The images or other third party material in this article are included in the article's Creative Commons license, unless indicated otherwise in a credit line to the material. If material is not included in the article's Creative Commons license and your intended use is not permitted by statutory regulation or exceeds the permitted use, you will need to obtain permission directly from the copyright holder. To view a copy of this license, visit <http://creativecommons.org/licenses/by/4.0/>.

© The Author(s) 2022